Dynamical behavior of a bistable chiral quasihomeotropic liquid crystal cell

Chih-Yung Hsieh and Shu-Hsia Chen

Articles you may be interested in

Dual-frequency addressed hybrid-aligned nematic liquid crystal
Appl. Phys. Lett. **85**, 3354 (2004); 10.1063/1.1809282

Electro-tunable laser action in a dye-doped nematic liquid crystal waveguide under holographic excitation
Appl. Phys. Lett. **83**, 422 (2003); 10.1063/1.1593827

Microwave liquid crystal wavelength selector
Appl. Phys. Lett. **79**, 3717 (2001); 10.1063/1.1419240

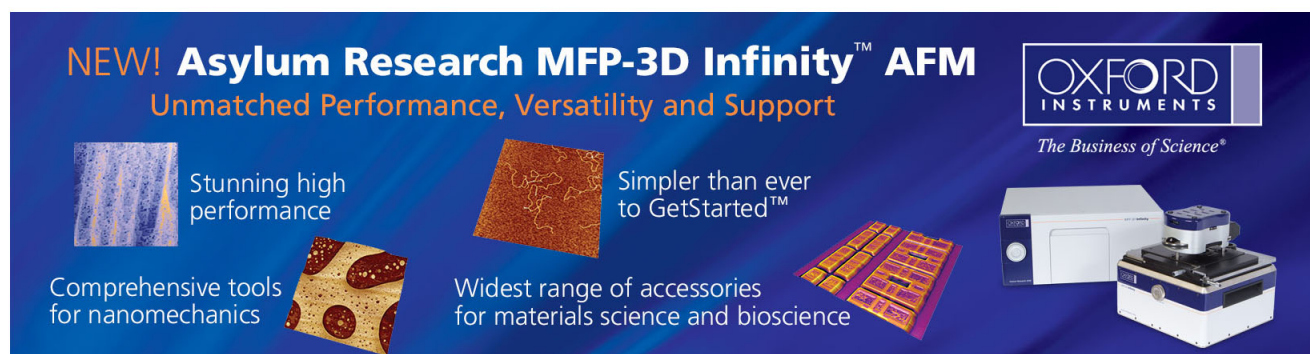Photoinduced in-plane switching of a photochromic nematic liquid crystal
J. Appl. Phys. **89**, 7730 (2001); 10.1063/1.1371944

Electrically assisted self-confinement and waveguiding in planar nematic liquid crystal cells
Appl. Phys. Lett. **77**, 7 (2000); 10.1063/1.126859

Dynamical behavior of a bistable chiral quasihomeotropic liquid crystal cell

Chih-Yung Hsieh[a)] and Shu-Hsia Chen
Institute of Electro-Optical Engineering, National Chiao Tung University, 1001 Ta Hsueh Road, Hsinchu 300, Taiwan, Republic of China

The dynamical behavior of the directors in a bistable chiral quasihomeotropic (BCQH) liquid crystal cell has been investigated. This cell can be switched from the initial quasihomeotropic configuration state at zero field to two static twisted states at 14 V by different switching processes. We studied the dynamic behavior of the BCQH cell based on the general nematohydrodynamic theory, and the detailed dynamical mechanism was illustrated by analyzing the director and velocity profiles obtained from the numerical simulation. We found that, in addition to the flow effect, the asymmetric polar-alignment condition is another important factor to achieve the switching bistability of our BCQH cell. The experimental and numerical results are reported in this letter. © *2003 American Institute of Physics.* [DOI: 10.1063/1.1600506]

Homeotropic liquid crystal (HLC) cells[1] are widely used in transmissive and reflective displays due to its excellent optical properties such as high contrast ratio.[2,3] Recently, our group[4] has demonstrated a chiral doped HLC device which can be switched into two different configuration states by controlling the switching process. However, the detailed dynamical mechanism of this device has not been well understood. In order to expand the application of this device, further studies on the configuration and dynamical transition of these states are necessary. For convenience, because the boundary directors are not precisely normal to the substrates, we named the devices bistable chiral quasihomeotropic (BCQH) devices.

In this letter, we studied the dynamical behavior of directors in the BCQH cell experimentally and numerically. The switching bistability of this cell was demonstrated. The initial quasihomeotropic state could be switched into two different static states by controlling the switching process. In addition, we also observed the appearance of another static state from the nucleation of a defect while we held the applied voltage about few minutes later. Furthermore, we studied the dynamical mechanism of our BCQH cell based on the Ericksen–Leslie theory by using a numerical method. We found that the switching bistability of this cell is realized by the fluid flow effect of directors together with the asymmetrical polar-alignment condition, which was usually ignored for a quasihomeotropic cell. Our simulation also indicated that the two static states are all twisted states whose effective helical axis tilted downward to different directions.

To study the dynamical mechanism of the BCQH cell, we made several samples to observe its transient behavior. The substrates were coated with a JALS-2021(JSR Co.) alignment layer, and the rubbing direction (*x*-axis) of top and bottom substrates was antiparallel. The liquid crystal material was ZLI-2806 (Merck Co.) and the cell gap was 5.88 μm. We added about 1 wt% of S811(Merck Co.) as chiral dopants to obtain a suitable helix pitch length. The light source was a 632.8-nm He-Ne laser, and the optical properties were measured under a cross-polarizer condition. The angle between the front polarizer and the rubbing axis was 45°, and the transient transmittance was detected by a photodiode and recorded by an oscilloscope.

Figure 1 shows the measured transient transmittance of the BCQH cell with two different driving wave forms whose amplitudes are both 14 V. According to the final transmittance, it is obvious that this cell can be switched from the quasihomeotropic state into two different static director states by controlling the switching process. In Fig. 1(a), wave form A has a gradual slew rate ($dV/dt=70$ V/s) and produces weak fluid flow. This weak flow effect drives the cell into the high-transmittance state. However, wave form B of Fig. 1(b), with a rapidly rising voltage, results in the strong flow effect of the directors and switches the cell into the low-transmittance state. This behavior occurs as long as the slew rate (dV/dt) is larger than 2.8 V/ms. Consequently, it can be found that the flow effect is the most important factor on the switching bistability in this cell. Besides, if we turn off the voltage 1 s after turn-on, both states will relax back to the quasihomeotropic state smoothly and continuously. However, it is worth noting that, if we hold the bias voltage for about 30 min, both states will transfer into an-
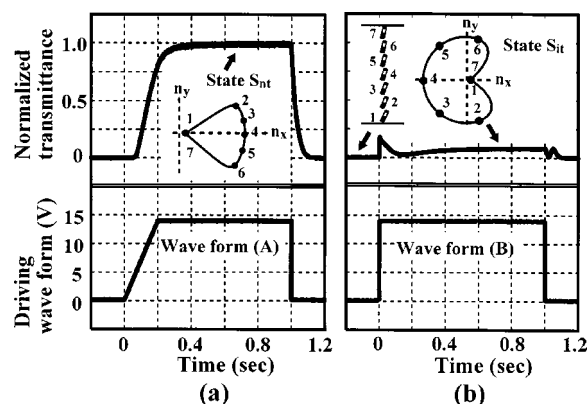

FIG. 1. Measured transient transmittance of BCQH cell with different driving wave forms. (a) The slew ratio of the wave form is $dV/dt=70$ V/s. (b) The wave form has rapidly rising voltage. The insets are the director configurations for quasihomeotropic state S_{nt} and S_{it} state.

[a)]Electronic mail: cjhsieh.eo88g@nctu.edu.tw

other state by the nucleation of a defect and the subsequent motion of a disclination line. Once we turn off the applied voltage, the new state does not relax back to the initial quasi-homeotropic state immediately, and the transition to the initial quasihomeotropic state is also caused by the same process as that of the appearance of this state. We believe the new state is a twisted 180° state. However, the mechanism of the state-transition process is not well understood.

By comparing the final transmittance of experimental and numerical results, we obtained the director configurations for these states; details of the simulation will be described later. The calculated static director profiles projected on the xy plane were plotted in the insets of Fig. 1. For easier imagining, one can regard these configurations as a conic helical structure with the effective helical axis of directors tilted downward toward the substrate, not normal to the substrate. Around the effective helical axis $\mathbf{L}$ the directors rotate a full turn from the bottom substrate to the top one. Therefore, the effective chiral property of LCs is consistent to the boundary condition of substrates. In the high-transmittance state, because the direction of the projection of $\mathbf{L}$ on the x-axis is the same with that of the boundary directors, we name this state the normal twisted state, denoted by $\mathbf{S}_{nt}$. However, in the low-transmittance state, the direction of the projection of $\mathbf{L}$ on the x-axis is inverse to the easy direction on the substrate, we name this state the inverse twisted state, denoted by $\mathbf{S}_{it}$. The transmittance of both $\mathbf{S}_{nt}$ and $\mathbf{S}_{it}$ states can be understood by the transmittance equation, $T = 0.5 \sin^2 2\psi \sin^2(\delta/2)$, for an uniaxial phase retarder between crossed polarizers, where ψ is the azimuthal angle between its optical axis and front polarizer, and δ is the phase retardation. When the phase retardation δ is fixed, the amplitude T is proportional to $\sin^2 2\psi$ and the maximum T happens at $\psi=45°$ or $135°$ due to $\sin^2 2\psi=1$. Therefore, the director configurations in the states $\mathbf{S}_{nt}$ and $\mathbf{S}_{it}$ can be regarded as the combination of a stack of subretarders with fixed δ and different ψ. Since the directors in the state $\mathbf{S}_{nt}$ are concentrated toward to the xz plane and the most azimuthal angles ψ are close to $45°$, the state $\mathbf{S}_{nt}$ has high transmittance. However, in the state $\mathbf{S}_{it}$, there are only a few directors whose ψ close to $45°$ or $135°$, and thus leading to low transmittance.

To analyze the dynamical switching mechanism of BCQH cells, we solved the hydrodynamic equations of LC from the Ericksen–Leslie theory[5–8] by using relaxation method and neglected the inertial term of directors. We assumed the surface as having rigid anchoring and neglected the surface divergence term for K_{13} and K_{24}. After calculating the transient director configuration, the transient transmittance was obtained by using Jones' matrix method. Table I shows the parameters used in our simulation for the cell with symmetric boundary conditions.

The calculated transient transmittances of our BCQH cell with different boundary conditions for driving wave forms A and B are shown in Fig. 2. Figure 2(a) indicates the results with wave form A, which can only induce a weak flow, for the symmetric and asymmetric polar-alignment cells. The top and bottom pretilt angles of the symmetric cell are both $85°$, but the bottom one in the asymmetric cell is $84°$. It is obvious that, as depicted in Fig. 2(a), the weak flow

TABLE I. Parameters used in the simulation. K_{ii} are the elastic constants. n_e and $\epsilon_\parallel$ are the extraordinary refractive and dielectric constants, respectively. Δn and $\Delta\epsilon$ are the optical and electric anisotropies, respectively. The six Leslie coefficients α_i are taken from MBBA.

Pitch	$-11.0 \ \mu$m	Tilt angle	85.0°
K_{11}	14.9 pN	Twist angle	0.0°
K_{22}	7.9 pN	α_1	-21.5 mPa s
K_{33}	15.4 pN	α_2	-153 mPa s
n_e	1.5183	α_3	-0.7 mPa s
Δn	0.0437	α_4	109.5 mPa s
$\epsilon_\parallel$	3.3	α_5	107 mPa s
$\Delta\epsilon$	-4.8	α_6	-46 mPa s

effect results in the symmetric and asymmetric cells driven into the $\mathbf{S}_{nt}$ state. Nevertheless, the asymmetric boundary condition will increase the final transmittance a little for the asymmetric cell. On the other hand, wave form B can induce a strong flow, as shown in Fig. 2(b), such that the asymmetric cell can be switched into the $\mathbf{S}_{it}$, and the calculated transmittance curve agrees with the measured results qualitatively. However, the symmetric cell cannot be switched into the $\mathbf{S}_{it}$ state and its final transmittance corresponding to the static state $\mathbf{S}_{nt}$. Therefore, the switching bistability cannot be achieved for the symmetric cell by controlling the flow effect of directors. This result indicates that there is an extra key factor, the asymmetric polar-alignment condition, for the switching bistability of our BCQH cell, except the flow effect. In our experiment, because it is very difficult to avoid the deviation between the top and bottom tilt angles the switching bistability cell can be observed.

The physical pictures of the switching dynamics for the symmetric and asymmetric cells with strong flow effect, as shown in Figs. 3 and 4, are described in the following. In the quasihomeotropic cell, the flow effect is induced by the external electric torque and depends on the initial director configuration.[9,10] The simulated velocity profiles at 0.5 ms after turn-on of the applied voltage for the symmetric cell are plotted in Fig. 3. The initial polar angle θ, that is, $\pi/2$ minus the tilt angle, of directors for the symmetric cell are the same to minimize the free energy. When the electric field is applied, the initial electric torque $\tau_{elec}=0.5\Delta\epsilon E_z^2 \sin 2\theta$, where E_z is the z-component of electric field, is the same for all directors owing to the same polar angle. Nevertheless, due to the rigid surface anchoring, the rotation of the directors results in an elastic deformation. The largest deformation occurs near the surfaces, and the smallest one is at the midplane
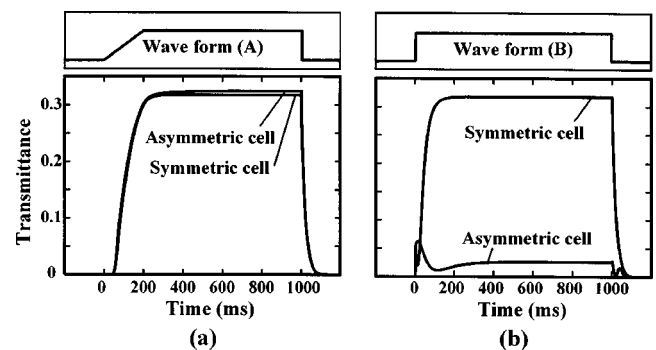

FIG. 2. Calculated transient transmittance of BCQH cell with symmetric and asymmetric cell for different driving wave forms. (a) Wave form A. (b) Wave form B.
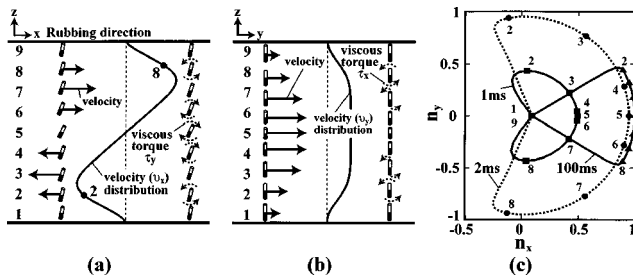
FIG. 3. Calculated flow velocity distribution at 0.5 ms after switching on the voltage for the symmetric cell. (a) v_x. (b) v_y. (c) Transient director configuration projected onto the xy plane.

because of the symmetric boundary condition. This deformation produces an elastic restoring torque to suppress the rotation of directors by the electric torque. Therefore, the mid-director has the fastest rotation because of the smallest restoring elastic torque, but the directors near the surface have the slowest rotation. This nonuniform rotation acts on the fluid element with different stress forces through viscous interaction and the net force causes a translational motion of the fluid elements. Meanwhile, the gradient of the flow velocity imposes a viscous torque $\boldsymbol{\tau}$ on the director, where $\boldsymbol{\tau} = (\tau_x, \tau_y, \tau_z) \approx (-|\alpha_2|n_z^2 v_{y,z}, |\alpha_2|n_z^2 v_{x,z}, 0)$ as a result of $n_z \gg n_x, n_y$ and $|\alpha_2| \gg |\alpha_3|$, $v_{x,z}$ and $v_{y,z}$ are the gradient of velocity, (n_x, n_y, n_z) are the components of director $\mathbf{n}$. Near the surface, at points 2 and 8 in Fig. 3(a), the viscous torque τ_y is negative, and that makes the director rotate in a direction opposed to the original one due to the elastic torque. This phenomenon is usually called the kickback effect. However, on the central part of the cell, the viscous torque τ_y is positive and speeds up the rotation of directors to tilt downward to the positive x-axis. At the same time, because the velocity gradient $v_{y,z}$ of the mid-director is zero, as illustrated in Fig. 3(b), the viscous torque τ_x has no influence on it; but near the top and bottom substrates, since the viscous torque τ_x has the inverse direction, it rotates the director near the surface out of the xz plane, causing a large elastic deformation. This large deformation introduces a restoring elastic torque, which pulls the director backward to the xz plane. Finally, the director profile reaches its static state $\mathbf{S}_{nt}$, as shown in Fig. 3(c).
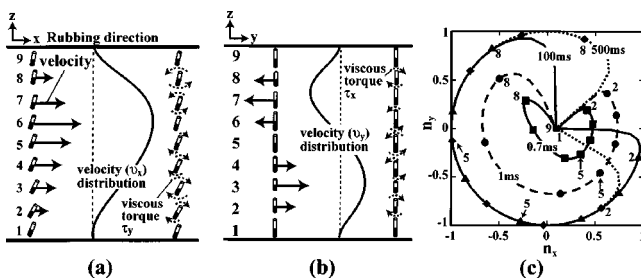
Figure 4 shows the simulated results of the asymmetric cell with a small polar angle θ at the top substrate that is less than the bottom one. The difference of polar angles causes a very small bend and twist distortion such that the initial director profile can be regarded as a helical structure with a very small conical angle. At the presence of the external field, the directors at the bottom boundary with the largest polar angle experience the biggest electric torque. In other words, the initial electric torque is asymmetric. It has to be emphasized that this cell is very different to the situation of the symmetric cell whose initial electric torque is symmetric. The asymmetric torque results in the peculiar director and velocity profiles. The simulated velocity distribution at 0.5 ms is illustrated in Fig. 4. As shown in Fig. 4(a), the velocity extreme of v_x happens near the midplane, and the viscous torque τ_y is negative on its upper side, but positive on the other side. Meanwhile, in Fig. 4(b), the τ_x is positive in the middle part of the cell, but negative in the region near two substrates. The resultant torque of τ_x and τ_y drives the directors in the bottom- and top-half parts into the first and second quadrants, respectively, and the mid-director into the fourth quadrant [see the 0.7-ms and 1.0-ms curves in Fig. 4(c)] to form a large heart-shaped loop. When the flow velocity of the fluid elements becomes small via viscous interaction, the director profile gradually swings clockwise into the state $\mathbf{S}_{it}$ by the twisted restoring elastic torque. Therefore, we concluded that the asymmetric polar-alignment condition is another important factor, in addition to the flow effect, for the switching bistability in our BCQH cell.

In summary, the switching bistability of the BCQH cell has been studied experimentally and numerically. From our numerical results, the realization of the switching bistability of our BCQH cell is achieved by the flow effect of directors together with the asymmetric polar-alignment condition. The two static states are all twisted states whose effective helical axis tilted downward in two different directions. Furthermore, we also observed the appearance of another state by nucleation of a defect. However, the detailed mechanism of the state transition is not understood and needs further investigation.

FIG. 4. Calculated flow velocity distribution at 0.5 ms after switching on the voltage for the asymmetric cell. (a) v_x. (b) v_y. (c) Transient director configuration projected onto the xy plane.

[1] M. F. Schiekel and K. Fahrenschon, Appl. Phys. Lett. **19**, 391 (1971).
[2] K. Ohmuro, S. Kataoka, T. Sasaki, and Y. Koike, *Soc. Inform. Display Tech. Digest*, 1997, p. 845.
[3] H. Kurogane, K. Doi, T. Nishihata, A. Honma, M. Furuya, S. Nakagaki, and I. Takanashi, *Soc. Inform. Display Tech. Digest*, 1998, p. 33.
[4] L. Y. Chen and S. H. Chen, Appl. Phys. Lett. **74**, 3779 (1999).
[5] J. L. Ericksen, Trans. Soc. Rheol. **5**, 23 (1961).
[6] F. M. Leslie, Arch. Ration. Mech. Anal. **28**, 265 (1968).
[7] C. Z. van Doorn, J. Appl. Phys. **46**, 3738 (1975).
[8] D. W. Berreman, J. Appl. Phys. **46**, 3746 (1975).
[9] L. Y. Chen and S. H. Chen, Jpn. J. Appl. Phys. **39**, L368 (2000).
[10] C. Y. Hsieh and S. H. Chen, Jpn. J. Appl. Phys. **41**, 5264 (2002).